Journal of Science and Technology Volume 48, Issue 4, 2010 pp. 153-165

ROAD BOUNDARY DETECTION USING SEGMENTATION ON STEREO IMAGES

T. T. SON, A. TAKEUCHI, S. MITA

ABSTRACT

In this paper, a road detection method based on an image segmentation and stereo vision is presented. Road detection process is a key issue for an autonomous driving system in urban environment. Image-based road detection algorithm is applied on sources of visual information recorded by stereo cameras when our car is running on road. Our method combines a posteriori probability and visual information for image segmentation. The depth map in stereo camera is calculated on real time by a circuit board and it is utilized to rectify the boundary on left and right side of road. The method is composed of three steps. Firstly, a road identifier is trained with supervised learning algorithm. Secondly, road regions are detected by combining a posteriori probability and visual information using image segmentation algorithm. In the last step, the segmentation result is combined with the depth-map image to correct the boundary. Experimental results are presented for video sequences of road in urban areas.

Keywords. SWA algorithm, Bayes's rule, depth map, road detection.

1. INTRODUCTION

Road detection plays an important role in autonomous driving system. Much of work on road detection was proposed and successfully demonstrated in the past[1, 6, 11, 15], especially before the Urban Challenges organized in 2007. There are two main approaches in the previous works: camera-based [2, 4, 8, 13, 21] and laser-range-based [5, 19, 20, 23] methods. In that system, road detection includes two stages: 1) Road boundary detection; 2) Road modeling. Road boundary detection returns the shape of road in one frame, a result in a 2D image. Meanwhile, road modeling process will receive these results of road boundary detection and transform them into a 3D map. In few works, there is an assumption that road plane is a flat surface. In this case, road modeling can be expressed on a 2D image as a parallel line or curve of boundaries. Otherwise, the result of this process must be a 3D shape of road boundaries. In much of work proposed recently [12, 17, 18], there are three necessary steps to solve this problem: feature extraction, modeling and curve fitting. Feature extraction proposes feature points in the road boundary and utilizes them as control points for modeling process. This process calculates the Inverse Perspective Mapping (IPM) to transform the coordinates of feature points from image plane to road plane. As mentioned above, the road plane can be a map in 2D or 3D coordinate based on the assumption of road surface. The curve fitting process utilizes the distribution of control points to fit them into a line or a curve where a car can run and track in following. Beside thats it is also necessary to detect and extract curvature accurately [25]. In practice, we need to integrate two cases (line and curve) in one module because it is not enough time to classify a road shape into a line or curve in urban road. In the camera-based approaches, some methods like [21] considered road boundary detection as a tracking of road border or road markings by employing intensity, color, and texture as a dynamic model of visual cues unique on the road surface. The other methods like [8] employ the known edge information from image processing for the estimation of road boundary. The majority of image-based tracking algorithms were reported successfully on day light. On the other hand, image segmentation algorithms were applied to classify road and non-road regions of video images on the basis of color and texture cues [2, 13]. In there, some methods used supervised learning algorithm [4, 19] to train classifiers which identify the road region or utilized stereo images to estimate the depth map of road[14]. However, overland error, a positive error, usually occurs in image-based methods. As a result, image-based road detection algorithm does not work properly in many changes of environments. Recently, multiple prominent teams of the DARPA Urban Challenge 2007 in California,USA, have applied laser sensors [9] to measure surrounding environment of autonomous car. Although this approach is robust and convenient to keep a car on road, it still lacks ``roadness" information and traffic signal. Here we call “roadness” a surrounding region where a car can move forward or backward safely and legally. In this paper, “roadness” is a region of road in front of car and it is recorded by a camera system mounted on the car bumper. For autonomous driving in our modern cities, we need an integration of camera-based and laser-sensor-based systems with a priori knowledge of surrounding environment. Without this condition, an autonomous driving car is similar to a system of autonomous driving train and it cannot work as it is being driven. In those challenges and efforts, a combination of laser-based and camera-based methods has been proved to be highly applicable in practice. In this paper, we propose a new method of the road detection from the camera-based point of view. Our proposed method provides a closed-form expression of an integration between visual information with an knowledge-based system of road: a priori probability of road and stereo vision for generating a robust system of road detection. This approach is also potentially applicable in robotic vision.

In this paper, we formulate visual information under a geometrical structure and utilize a priori knowledge of road to calculate a posteriori probability of ``roadness" through the Bayes's formula. A posteriori probability of road is applied as an extra information to reduce the ambiguity of the conventional segmentation algorithm in road detection. Then, the depth map is apply to rectify the segmentation result and return a correct road boundary. The structure of this paper is as follows; Section 2 reminds image segmentation methods; Section 3 describes our proposed method using image segmentation with a posteriori probability of ``roadness" and principle lines of depth-map images; Section 4 presents our simulation results; and Section 5 is the conclusions.

2. OVERVIEW OF SEGMENTATION ALGORITHM

The proposed algorithm is based on Segmentation by Weighted Aggregation (SWA) algorithm [22] that is a bottom-up image segmentation algorithm. The SWA algorithm constructs a weighted graph in which every pixel is a node and is connected to its neighboring pixels by an edge. A weight is associated with each edge reflecting the intensity contrast in the corresponding position in image. SWA algorithm produces a multi-scale and hierarchical graph representation of the image. The resulting segmentation takes texture (average intensity)into account regional properties. SWA algorithm finds the best partition from the constructed graph according to a saliency measure (related to a normalized-cut measure). The saliency is the segment's dissimilarity of its surrounding, divided by its internal homogeneity. We briefly describe the SWA algorithm as follows;

In the SWA algorithm, a 4-connected weight graph $G = (V, W)$ is constructed from the image, where each node $v_i \in V$ represents a pixel and each pair of neighbors are assigned coupling values as weight $w_{ij} \in W$. The initial weight reflects the intensity contrast between the two pixels i and j

$$w_{ij} = e^{-\alpha|I_i - I_j|} \tag{1}$$

where I_i and I_j denote intensities of two neighboring pixels, and α is a positive constant. Every segment $S = \{v_1, v_2, \ldots, v_m\} \subseteq V$ is associated with a state vector $u = (u_1, u_2, \ldots, u_n)$, where $N = PVP$, and u_1 is defined initially as follows;

$$u_i = \begin{cases} 1 \; if \; v_i \in S \\ 0 \; if \; v_i \notin S \end{cases} \tag{2}$$

SWA algorithm provides a fast transformation for coarsening a graph. Result of coarsening process is a pyramid structure, where the top of pyramid has the least number of salient segments. The coarsening process runs recursively by aggregating weights as follows;

Let $G^{[0]}$ denote a graph at initial level $(s = 0)$. Given a graph $G^{[s-1]}$ and a state vector $u^{[s-1]}$ at level $s - 1$, a set or representative nodes $V^{[s]} \subseteq V^{[s-1]} = 1,2, \ldots, N^{[s-1]}$ is chosen so that every node in $V^{[s-1]} - V^{[s]}$ is strongly connected to $V^{[s]}$. A node is considered strongly connected to representative node $V^{[s]}$ if the sum of its weight to representative nodes is a significant proportion of its total weight. Graph $G^{[s]} = (V^{[s]}, W^{[s]})$ at level s is generated by a weighted aggregation [22], where the weight $W^{[s]} = w_{kl}^{[s]}$ can be computed through $\overline{W}^{[s]}$.

$$\overline{W}^{[s]} = [\mathcal{P}^{[s-1,s]}]^T W^{[s-1]} \mathcal{P}^{[s-1,s]} \tag{3}$$

where $\overline{W}^{[s]} = \{\overline{w}_{kl}^{[s]}\}$, and $P^{[s-1,s]} - \mathcal{P}$ is called inter-scale interpolation matrix. To reduce complexity, the computation of the internal weight does not appear in eq. (3). $\mathcal{P}^{[s-1,s]}$ satisfies the following conditions

<u>Cond #1</u>: $\{P_{i,k}\}_{k=1}^{N^{[s]}}$ are chosen to be proportional to $\{w_{i,k}^{[s-1]}\}_{k=1}^{N[s]}$ for $\forall i \notin V^{[s]}$ and satisfy $\sum_k p_{ik}^{s-1,s} = 1$ for every i

<u>Cond #2</u>: $p_{ii}^{[s-1,s]}$ and $p_{ij}^{[s-1,s]} = 0$ for $i \in V^{[s]}$

To avoid a weak structure of weights provided by eq. (3), a modification is applied to update weight $\overline{W}^{[s]}$:

Given an aggregate k at scale s, let $\overline{Q}^{[s]}$ denote a weighted average of a property $a = (a_1, a_2, ., a_N)$. If the interpolation matrix $\mathcal{P}^{[s-1,s]}$ is given, the regional properties are computed recursively using the following equation

$$\overline{Q}^{[s]} = \frac{a_\cdot \mathcal{P}^{[0,1]} \ldots \mathcal{P}^{[s-1,s]}}{1^T \mathcal{P}^{[0,1]} \mathcal{P}^{[s-1,s]}}. \tag{4}$$

If we set a to be intensity of pixels, then we obtain the average intensity of an aggregation. These regional properties are utilized to modify weights. Then, weights in new graph are modified to incorporate coarse measure of the differences between neighboring aggregates as follows;

$$w_{kl}^{[s]} = \overline{w}_{kl}^{[s]} \times \exp\left(-\gamma|\overline{Q}_{k}^{[s]} - \overline{Q}_{i}^{[s]}\right) \tag{5}$$

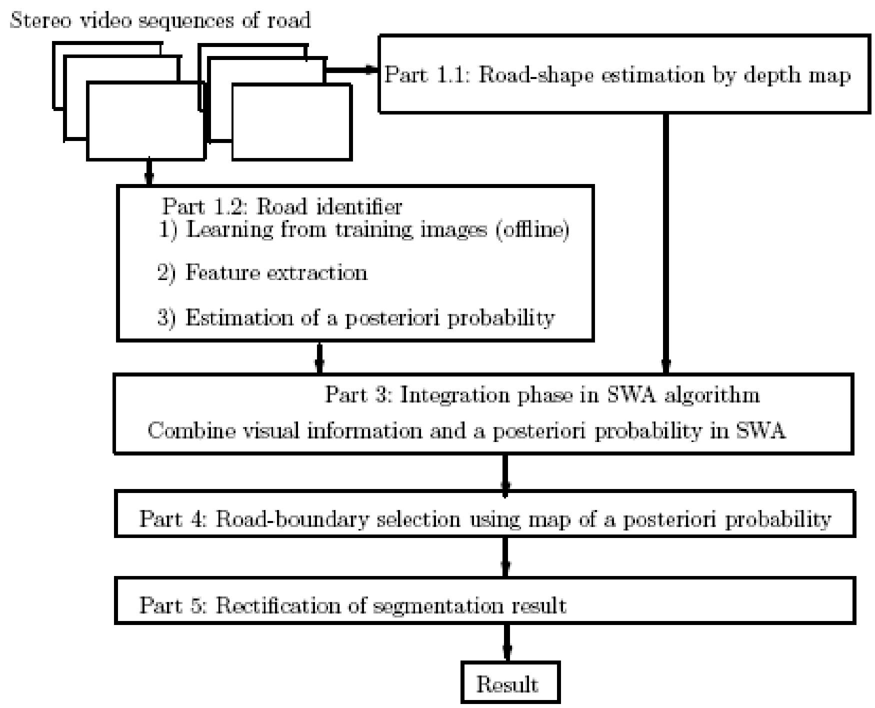

Figure 1. Proposed method

where γ is positive. The weight w_{kl} takes a decrease if there is a difference between regional properties $Q^{[s]}$. This coarsening procedure is repeated recursively. As a result, a full pyramid structure of the image is constructed. Coarsening measurement utilizes weight to reflect the multi-scale regional properties [7] during the construction of the pyramid. In this algorithm, coarsening measurement is used to facilitate the segmentation process.

After coarsening graph, sparse matrix $P^{[s-1,s]}$ is recorded and utilized in sharpening process as follows;

$$u^{[s-1]} \approx P^{[s-1,s]} u^{[s]}, \tag{6}$$

where $u^{[s-1]} = \{u_i\}_{i=1,...}$ $u^{[s-1]} = \{u_i\}_{i=1,...}$ is selected as follows;

$$u_i = \begin{cases} 1 \ if\ u_i > 1 - \delta_2 \\ u_i \ if\ \delta_1 \leq u_i \leq 1 - \delta_2 \\ 0 \ if\ u_i < \delta_1 \end{cases} \tag{7}$$

where values δ_1 and δ_2 are two thresholds of state values.

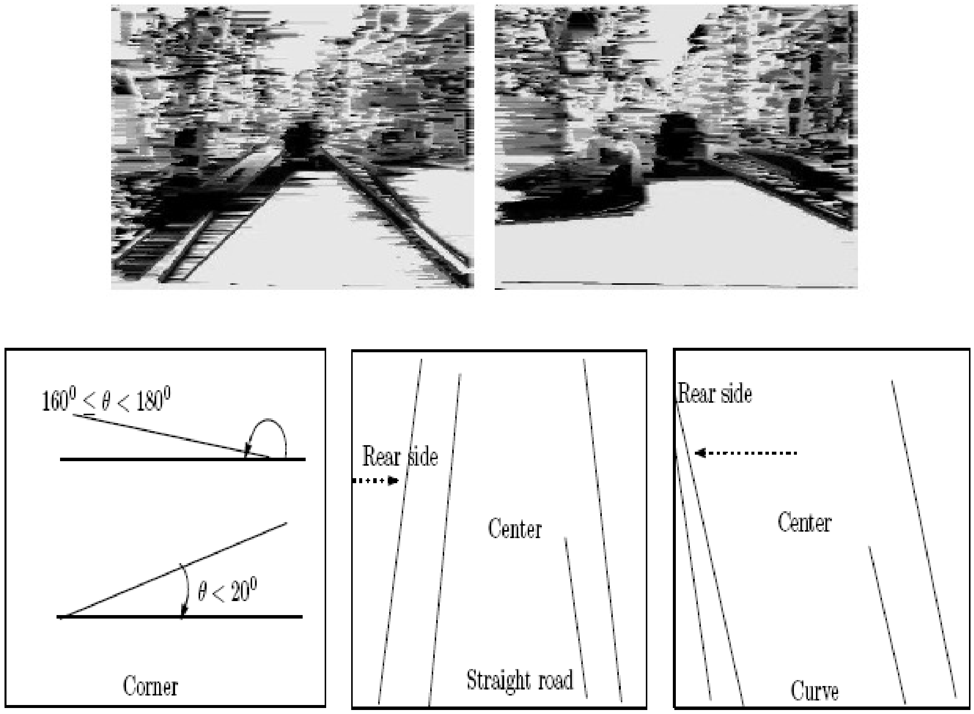

[Straight road in depth map] [Corner in depth map] [Principle lines in road map]

Figure 2. Line detection on depth-map images.

3. ROAD BOUNDARY DETECTION

We utilize a condition of road shape as a priori knowledge and depth map as the first information in real-time estimation. Figure 1 presents our designed system for road boundary detection. In Part 1.1, a line-detection process is applied to find the main line which has a shape of road based on its direction. In Part 1.2, a posteriori probability of road region is calculated on each block of image and it is utilized as a condition to select results of SWA segmentation. In this system, the depth map is calculated on real-time by a circuit board in camera system. There are two kinds of principle lines in road image: horizontal line, and vertical line. The vertical line has a direction from rear to center of image and the horizontal line usually has a tilt direction from bottom to top of image. When the distribution of horizontal line appears more frequently, a corner or a cross street may be in front of the car. Similarly, if the distribution of vertical line in which its direction is from center to rear instead of rear to center appears more frequently, the car may come into a curve. Figure 2 presents one of our principle line detection on the depth-map images. The Hough transform is applied for line detection. Our camera system can provide a processing time of 10 fps for depth map and line detection with the image size of 320×240.

3.1. Road Identifier

We assume that an image taken in the urban environment is composed of two regions: the road region and the non-road region. This problem is a two-category classification. Let ω denote one state in practice, with $\omega = \omega_1$ for road and $\omega = \omega_2$ for non-road at one rectangle $\emptyset$ of size $\ell \times \ell$ in input image. Let $P(\omega)$ denote a priori probability, where $P(\omega_1) + P(\omega_2) = 1$. A priori probability $P(road)$ is calculated from a training data set. A priori probability of one road image is segmented into 3 regions. In the top region, $P(road)$ is always set to 0. In the middle region, $P(road)$ is larger or equal to 0 and less than or equal to 1. In the bottom region, $P(road)$ is always set to 1. It means that it is not necessary to consider a posteriori in the top and bottom regions of training results because the probability is set to 0 and 1, respectively. This is presented by some samples in Fig. 3.

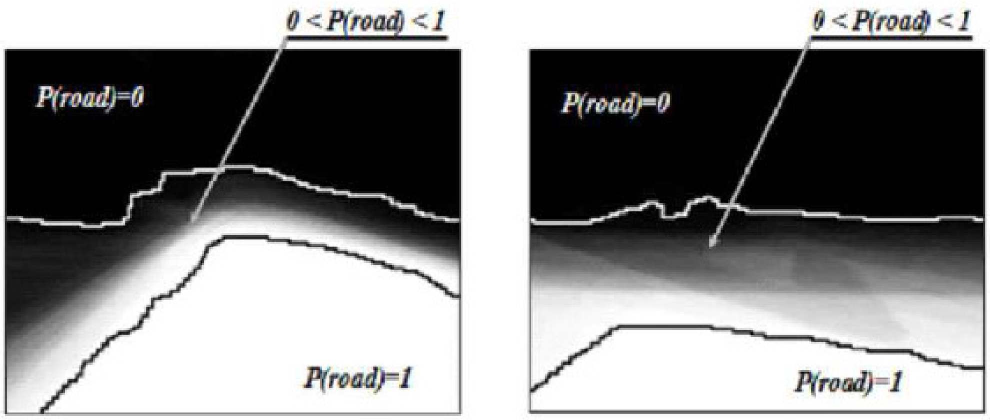

Figure 3. Probability of road region.

In the feature extraction process, we utilize moving average variance of intensity obtained from samples of video sequences. The average variance σ^2 is utilized as a feature of our road-detection process because the boundary of road in the average-variance images is clearer than that in the average intensity does. This process is calculated from sequential images as follows;

The variance of the x^{th} frame at position (i, j) is calculated using an average value of n previous frames as follows;

$$\sigma_{ij}^2 = \frac{1}{n}\sum_{k=0}^{n-1}\left(I_{ij}(x-k) - \bar{I}_{ij}(x)\right)^2 \tag{8}$$

$$\bar{I}_{ij}(x) = \frac{1}{n}\sum_{k=0}^{n-1} I_{ij}(x-k) \tag{9}$$

where $I_{ij}(x)$ is the intensity of x^{th} x^{th} frame at position (i, j).

3.2. A posteriori probability of road regions

We can estimate a posteriori probability $P(\omega|\sigma^2)$ according to the Bayes formula if the value of σ^2 has been measured. The road identifier is described as a posteriori probability of road region on condition of variance

$$P(\omega_1|\sigma^2) = \frac{P(\sigma^2|\omega_1)P(\omega_1)}{P(\sigma^2|\omega_1)P(\omega_1)+P(\sigma^2|\omega_2)P(\omega_2)} \quad (10)$$

Similarly, a posteriori probability of non-road class is

$$P(\omega_2|\sigma^2) = \frac{P(\sigma^2|\omega_2)P(\omega_2)}{P(\sigma^2|\omega_1)P(\omega_1)+P(\sigma^2|\omega_2)P(\omega_2)} \quad (11)$$

where $P(\sigma^2|\omega_1)$ is the likelihood probability function of class $\{\omega_i\}_{i=1,2}$. In this case, we have estimated them by using a non-parametric approach to estimate the probability density function from training data. It is noted that non-parametric approach can be used for arbitrary distribution no matter how the forms of the underlying densities change.

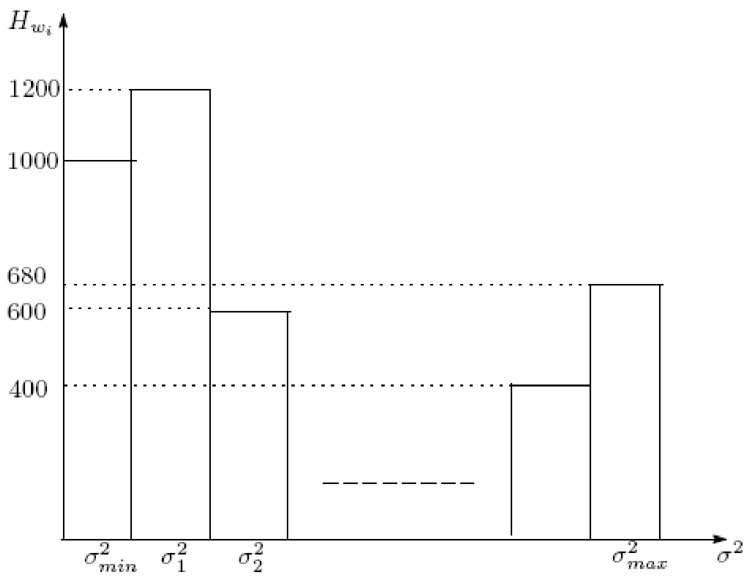

Figure 4. Histogram at position of rectangle ϕ

We consider boundaries of road and non-road regions where their priori probability is larger than 0 and less than 1. $P(\sigma^2|\omega_i)$ is calculated by using information from both ground truth and variance images. Each sample image in learning step is divided into many small rectangles $\emptyset$ of the size $\ell \times \ell$ and calculate the likelihood probability $P(\sigma^2|\omega_i)$ for each rectangle $\emptyset$ instead of working on each position of pixel. For each position of rectangle $\emptyset$, we generate two histograms, one for road and another for non road, by using ground truth and variance image to count the number of pixels in all learning samples. Normalization of two histograms H_{ω_i} corresponding to position of $\emptyset$ gives us a likelihood probability $P(\sigma^2|\omega_i)$. Figure 4 presents one histogram H_{ω_i} counted on all learning samples at position of rectangle $\emptyset$.

3.3. Integration phase

In the conventional SWA algorithm, it is not necessary to utilize feature information. Our proposed method is a modification of SWA by combining visual information and a posteriori probability of road. This helps to improve accuracy of segmentation considerably in road detection. Let $a = \mathcal{R}^{[0]} = (\mathcal{R}_1, \mathcal{R}_2, \ldots, \mathcal{R}_N)$ denote a set of road region probability. Here R_i denotes an output of the road identifier at position i, and N denotes the number of the pixels of the input image. The average road region is calculated by the following condition;

$$\hat{R}^{[s]} = \frac{\mathcal{R}^{[0]} P^{[0,1]} \ldots \mathcal{P}^{[s-1,s]}}{1^T \mathcal{P}^{[0,1]} P^{[s-1,s]}}. \tag{12}$$

We use intensity of the image as visual information, and also use the road-region probability of the road identifier. In the construction of a new level of s, the weight is generated according to using a fine-scale weight and interpolation matrix. We modify $w_{kl}^{[s]}$ to account for similarity of the road region between two aggregates k and l as follows;

$$w_{kl}^{[s]} = \overline{w}_{kl}^{[s]} e^{(-\lambda |\hat{R}_k^{[s]} - \hat{R}_l^{[s]}|)}. \tag{13}$$

In practice, we can combine more information from average intensity, road region, and result of previous frame for calculating frame. The equation (13) is modified as follows;

$$w_{kl}^{[s]} = \overline{w}_{kl}^{[s]} e^{(-\alpha_1 |I_k - I_l|)} \times e^{(-\gamma |\hat{R}_k^{[s]} - \hat{R}_l^{[s]}|)} \times e^{(-\alpha_2 |\hat{S}_k - \hat{S}_l|)} \tag{14}$$

where $\overline{I}_k$ is the average intensity of image at level k and $\hat{S}_k$ is the segmentation result of previous frame at level k. In this process, an image is given as input and the a priori road identifier has been trained. Firstly, the feature of σ^2 is extracted from sequential input images for each pixel and we estimate its probability of road region from the road identifier. Secondly, a fitness level graph is generated for the SWA algorithm. Then, weights at the finest-level graph are the intensity contrast. During the coarsening procedure, the average road region of the aggregates is calculated by fine-tuning weights between them. This procedure allows the neighboring aggregates of similar road region to merge at the next levels of the coarsening process and permits the aggregates of different road region to stand out.

3.4. Road-boundary selection and rectification

Results of road segmentation process is corrected by using results of learning phase and the principle lines of depth-map images. Based on feature σ^2 of the current frame, $P(\sigma^2|\omega_i)_{i=1,2}$ is calculated to provide a map of probability for each block in the current frame. To keep the smoothness boundary of road, we combine principle lines of depth-map images with result of the SWA algorithm at the lower level of the pyramid. In practice, we select the lower level s until there ia a boundary which can be matched to the principle lines of depth-map image. Then, the boundary of road is selected by the average probability of road region in each segmented regions. If the average probability value of one saliency is larger than a threshold ρ, it will be recorded as a road region. Otherwise, it is a non-road region. This is described in eq. (15) as follows;

$$\zeta(S_k) = \begin{cases} road - region, E[P(road|\sigma^2)]_{S_k} > \rho \\ non - road - region, Otherwises \end{cases} \tag{15}$$

where $\zeta(\cdot)$ is a classification function of road region and non-road region, and $E[\cdot]_{S_k}$ is an expectation of $P(road|\sigma^2)$ calculated in a saliency S_k. This step is useful to prevent large error which usually appears in the two-segment results, road and non-road, of the SWA algorithm. Figure 5a presents a result of two-segment level in the SWA algorithm. There is error in the left side of the image caused by weighted aggregation as shown in Fig. 5b. Figure 5b describes a result of the SWA algorithm for a level of $s = 8$, where the principle lines of depth map is matched to segmentation boundary. Figure 5c presents a map of a posteriori probability with its segmented regions for the current frame. In Fig. 5c, the average probability of $P(road|\sigma^2)$ is presented for each segmented region S_k. Figure 5d describes the final result of segmentation. Its regions are correspondent to saliencies of the map of a posteriori probability in Fig. 5c such that its average probability is larger than a threshold ρ and it belongs to the road region of Fig. 5a.

a) Two-segment result

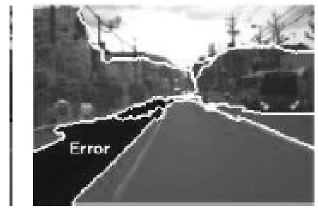

b) Multi-segment result matched to principle line of depth map

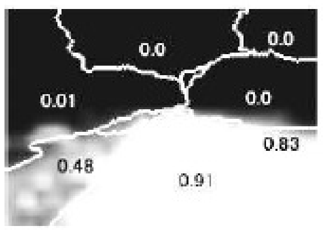

c) Probability map of segments

d) Final result

Figure 5. Sample result of rectification

4. SIMULATIONS

In simulation, our proposed method is applied into video sequences with 10 frames per second. Images in video sequence are gray scale image with the size of 184 × 130.

Table1. Parameters

Parameter	Value
δ_1	0.25
δ_2	0.25
α_1	4
r	7
α_2	2
ρ	0.6

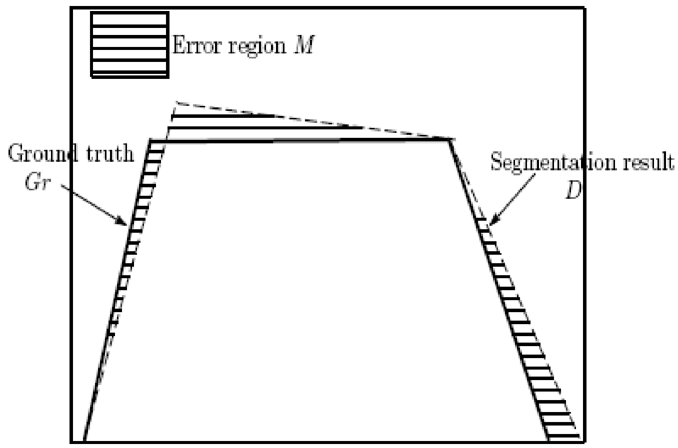

Figure 6. Error calculation

In the set of ground truth using in learning step, there are 50 pictures for turning left road, 50 pictures for turning right, and 30 pictures for running straight. We use k-mean algorithm to classify small rectangles of ground truth images into road and non-road classes based on their intensity. After that, a normalization on the distribution of road and non-road patches for each position in the size of 184 × 130 is applied to get a priori probability $P(road)$. This process takes 168.4 second. In eq. (14), the values of α_1, r, α_2, and ρ are set to 4, 7, 2, and 0.6, respectively. The value of r plays an important role for road information, and the value of ρ is the lower bound of road-region probability. The selection of ρ value is based on the probability values of all road patches in training process. If it is larger, the segmentation of road region is more confident and its boundary is also smaller. We have observed influences of parameter r to our algorithm in many video sequences with a total length of 12 minutes and a video rate of 10 frames per second. Table 1 presents a summary of all parameter values. The error of our method is calculated as follows;

$$Error = \frac{|M|}{|L|} \tag{16}$$

where $M = (D \cup Gr) - (D \cap Gr)$ and it denotes error regions, Gr denotes road regions in the ground truth generated manually, D denotes the road region of segmentation result, and L denotes the whole image. The operator $|z|$ returns the number of pixels belonging to region $|z|$. It is noticed that these parameters mentioned above express an important degree of information in weighting of segmentation. The changes of surrounding environment will affect to one parameter ρ only. In our experiments, ρ is set to 0.6 for sunny conditions. It should be set to a value larger than 0.6 when the front light of car is turned on. Figure 6 presents one sample of the ground-truth boundary Gr, segmentation result D and error regions M. Results corresponding to some frames in our experimental video are presented in Fig. 7. Figure 7*(a)* presents the original image with the road boundary in the ground truth. Figures 7(b) to 7*(e)* present the segmentation results corresponding to some changes of r.

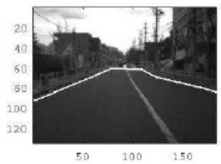

a) Ground truth

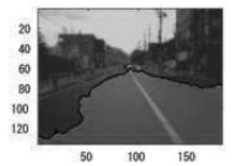

b) r = 3, Error = 11,7%

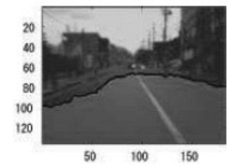

c) r = 7, Error = 3,7%

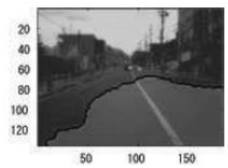

d) r = 10, Error = 11,1%

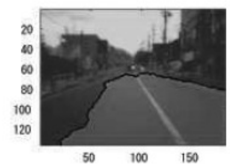

e) r = 15, Error = 10,3%

Figure 7. Varying parameter of *r*

It shows that the average error of road segmentation is smaller than 6.3% when the value of r is equal to 7. In practice, an autonomous driving car must have a GPS device to locate its position on road map. The GPS system, steering angle sensor, and road map recorded in car navigation will help our algorithm estimate the next direction of car movement. Our method takes 300 ms per frame by the Matlab program with a CPU of Dual-Core Xeon 3.0 GHz. In the C program, it takes an average time of 126 ms per frame. Table 2 presents a comparison with the previous work using single camera in road detection. Our proposed method can return a correct boundary and integrate information from many other sources easily. From our point of view in practice, road detection problem could not be solved completely by using only one picture of a single camera. The common errors are overland boundary and not excluding vehicles on road region. Therefore, we utilize the source of information coming from the previous frames and road patterns. It is shown that we can combine many sources of information easily to improve robustness and accuracy of road detection based on segmentation method. Comparison of road-detection methods using only single camera

Methods	Merit	Drawbacks
Jeong et.al.[10]	- Low complexity (0.02 s, 160 × 160)	- Incorrect boundary
Lombardi et.al.[13]	- Correct boundary	- High complexity and not excluding vehicle on road
Sha et.al.[24]	- Low complexity	- Not clear boundary and sensitive with shadow
Proposed method	- Correct boundary, excluding vehicle on road, integrating information easily	- High complexity (0.126 s, 184 × 130)

5. CONCLUSIONS

We have proposed a road detection method based on image segmentation algorithm. Our proposed method is a combination of visual information in stereo images and a posteriori probability for the detection of road in the urban environment. The proposed method has been applied on many video sequences under varying urban road condition and returns a robust result in varying illumination, environment, and shape of road. In those results, vehicles on road are also classified correctly without any post- or pre-process. Moreover, it is easy to integrate many other source of information such as data of GPS and laser range sensor into our proposed method to make a robust and confident system of road detection.

Acknowledgment. This work was supported by the Research Center for Integration of Advanced Intelligent Systems and Devices, Toyota Technological Institute, Japan. We also thank Toyota Central R&D Labs Inc. for data supplies and discussions.

REFERENCES

1. M. Betrozzi, A. Broggi, and A. Fascioli, Vision-based intelligent vehicles: State of the art and perspectives - Journal of Robotics and Autonomous Systems, 2000, pp. 1-16.
2. J. Crisman and C. Thrope - UNSCARF A color vision system for the detection of unstructured roads, Proc. Int. Conf. on Robotics and Automation, 1991, pp. 2396-2501.
3. C. Demonceaux, A. Potelle, and D. K. Akkouche - Obstacle Detection in a Road Scene Based on Motion Analysis, IEEE Trans. on Vehicular Technology **53** (6) (2004) 1649-1656.
4. M. Foedisch, and A. Takeuchi - Adaptive real-time road detection using neural networks, Proc. IEEE Conf. on Intelligent Transportation Systems, 2004, pp. 167-172.
5. B. Fardi, U. Scheunert, H. Cramer, and G. Wanielik - Multi-modal detection and parameter-based tracking of road borders with a laser scanner, Proc. IEEE Intelligent Vehicles Symposium, 2003, pp. 95 - 99.
6. Guilherm N. DeSouza, and A. C. Kak - Vision for mobile robot navigation: A survey, IEEE Trans. on Pattern Analysis and Machine Intelligence **24** (2) (2002) 237-267.
7. M. Galun, E. Sharon, R. Basri, and A. Brandt - Texture segmentation by multiscale aggregation of filter responses and shape elements, Proc. IEEE Conf. on Computer Vision and Pattern Recognition, 2003, pp. 716-723.
8. Y. He, H. Wang, and B. Zhang, Color-based road detection in urban traffic scences, IEEE Trans. on Intelligent Transport System **53** (4) (2004) 309-318.
9. B. Jenkin - Darpa Urban Challenge: Innovation Seedbed for 3D Laser Scanning, The American Surveyor, Feb. 2008.
10. P. Jeong, S. Nedevschi - Efficient and Robust Classification Method Using Combined Feature Vector for Lane Detection, IEEE Trans. on Circuits and Systems for Video Technology **15** (4) (2005) 528-537.
11. V. Kastrinaki, M. Zervakis, K. Kalaitzakis - A survey of video processing techniques for traffic applications, Journal of Image and Vision Computing (Elsevier) **21** (4) (2003) 359-381.
12. R. Labayrade, J. Douret, D. Aubert - A Multi-Model Lane Detector that Handles Road Singularities, Proc. IEEE Conf. on Intelligent Transportation Systems, 2006, pp. 1143 - 1148.
13. P. Lombardi, M. Zanin, S. Messelodi - Switching Models for Vision-based On-Board

Road Detection, Proc. IEEE Conf. on Intelligent Transportation Systems, 2005, pp. 67-72.

14. P. Lombardi, M. Zanin, S. Messelodi - Unified Stereovision for Ground, Road, and Obstacle Detection, Proc. IEEE Conf. on Intelligent Vehicles, 2005, pp. 783-788.
15. J. C. McCall M. M. Trivedi - Video-based lane estimation and tracking for driver assistance: survey, system, and evaluation, IEEE Trans. on Intelligent Transport System **7** (1) (2006) 20-37.
16. M. Nieto, J. Arrospide, L. Salgado, F. Jaureguizar - On-board Video based System for Robust Road Modeling, Proc. IEEE International Workshop on Content-Based Multimedia Indexing, 2008, pp. 109-116.
17. M. Nieto, L. Salgado, F. Jaureguizar - Robust Road Modeling based on a Hierarchical Bipartile Graph, Proc. IEEE Intelligent Vehicles Symposium, 2008, pp. 61-66.
18. M. Nieto, L. Salgado, F. Jaureguizar, J. Cabrera - Stabilization of Inverse Perspective Mapping Images based on Robust Vanishing Point Estimation, Proc. IEEE Intelligent Vehicles Symposium, 2007, pp. 315-320.
19. C. Rasmussen - Combining laser range, color, and texture cues for autonomous road following, Proc. Int. Conf. on Robotics and Automation, 2002, pp. 4320-4325.
20. A. V. Reyher, A. Joos, H. Winner - A lidar-based approach for near range lane detection, Proc. Conf. on Intelligent Vehicles Symposium, 2005, pp. 147-152.
21. T. Suttorp, T. Bucher - Learning of Kalman Filter Parameters for Lane Detection, Proc. IEEE Intelligent Vehicles Symposium, 2006, pp. 552- 557.
22. E. Sharon, A. Brandt, and R. Basri - Segmentation and boundary detection using multiscale intensity measurements, Proc. IEEE Conf. on CVPR, Vol. 1, 2001, pp. 469-476.
23. J. Sparbert, K. Dietmayer, D. Streller - Lane detection and street type classification using laser rangeimages, Proc. IEEE Conf. on Intelligent Transportation Systems, 2001, pp. 454-459.
24. Sha Yun, Zhang Guo-ying, Yang Yong - A Road Detection Algorithm by Boosting Using Feature Combination, Proc. IEEE Intelligent Vehicles Symposium, 2007, pp. 364-368.
25. C. Wang, Z. Hu, K. Uchimura - Precise Curvature Estimation by Cooperating with Digital Road Map, Proc. IEEE Intelligent Vehicles Symposium, 2008, pp. 859-864.

Address:

Received June 16, 2010

Dept. of Electronics and Information

Toyota Technological Institute, Nagoya, Japan.